JACS
JOURNAL OF THE AMERICAN CHEMICAL SOCIETY
Communication
pubs.acs.org/JACS

Li/Mo Codoping of CaO Films: A Means to Tailor the Equilibrium Shape of Au Deposits

Xiang Shao, Niklas Nilius,* and Hans-Joachim Freund

Fritz-Haber-Institut der MPG, Faradayweg 4-6, D-14195 Berlin, Germany

ABSTRACT: Using scanning tunneling microscopy, we have investigated how the doping of CaO thin films affects the growth behavior of gold. Whereas 3D deposits develop on pristine films, 2D islands form after inserting 4% of Mo into the CaO lattice. Adding small amounts of Li to the Mo-doped CaO reinstalls the initial 3D growth regime. We assign this morphology crossover to charge transfer processes between the dopants and the ad-metal. Whereas Mo acts as an electron donor and provides excess charges to be transferred into the gold, Li creates electron traps in the oxide lattice that interrupt the charge flow toward the metal. The different Au charge states in the presence of the dopants are derived from different growth morphologies with anionic gold favoring a 2D mode due to an enhanced interface adhesion. Our work demonstrates how oxide doping can be exploited to tailor the equilibrium geometry of ad-particles on supported metal catalysts.

The performance of metal particles in heterogeneous catalysis is closely related to their size and morphology as well as to interactions with the oxide support.[1−4] Several authors have highlighted the particular relevance of flat metal deposits for various reactions. Goodman et al., for example, found bilayer Au rafts on titania thin films to be an order of magnitude more active in low-temperature CO oxidation than their mono- or multilayer equivalents.[5] A similar conclusion was drawn from an electron microscopy study on Au/FeO_x catalysts.[6] Also in the propanol oxidation over alumina-supported Pt, raft-like particles turned out to be the most reactive.[7] An explanation for the pronounced shape-dependence of metal particles in catalysis is the specific role of the particle perimeter that enables a simultaneous interaction of adsorbates with the metal and the oxide support.[8−10]

Given the importance of the particle geometry, several attempts have been made to tailor the shape of metal deposits on oxide supports.[11] On most bulk oxides, the growth of ad-metals follows the Volmer−Weber regime, resulting in compact 3D particles with large height to diameter (aspect) ratios. This growth behavior is governed by the inert nature of the oxide that only allows for a weak metal−oxide adhesion. A 2D growth of metals has been found on a few strongly interacting systems, e.g. on polar[12] and highly defective oxide surfaces.[13] The formation of monolayer islands is also revealed on various thin-film supports, where a spontaneous charge transfer into the ad-islands reinforces the metal−oxide adhesion.[4,14,15] However, all approaches for shaping metal deposits presented so far are restricted to specific oxide systems and therefore unsuitable to optimize particle geometries on conventional bulk oxides, as used in heterogeneous catalysis.

This work demonstrates how doping of an oxide material might be exploited to control the equilibrium shape of metal ad-particles. For this purpose, we have prepared CaO films of 50 ML thickness via Ca vapor deposition onto a Mo(001) single crystal in 5×10^{-7} mbar of O_2.[16] The doping was performed by adding defined quantities of Li and/or Mo to the reaction gas used for film preparation. Whereas Li is an undervalent dopant, Mo adopts a higher charge state than the initial Ca^{2+} and thus acts as electron donor. To avoid segregation of the dopants to the surface, the films were capped with 10 layers of pristine CaO. This particular thickness was chosen to enable diffusion of the dopants into a near-surface region without enriching them on top of the oxide layer. The preparation was completed by annealing of the film to 900 K in ultrahigh vacuum in order to stimulate its crystallization. Higher temperatures were avoided as they triggered Li desorption from the film.[17]

Four different samples have been prepared in this way, namely pristine CaO, Mo-doped (CaO_{Mo}), Li-doped (CaO_{Li}), and codoped (CaO_{LiMo}) films. They all display a sharp (1×1) LEED pattern as well as atomically flat and defect poor surfaces in low-temperature STM measurements (Figure 1a). The main

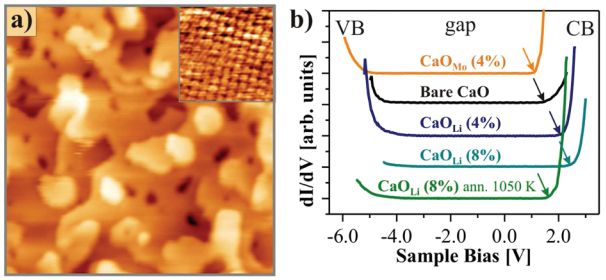

Figure 1. (a) STM image of a 50 ML thick Li-doped CaO film grown on Mo(001) (6.0 V, 50 × 50 nm^2). The inset shows an atomically resolved image of the CaO surface. (b) STM conductance spectra taken on pristine, Li- and Mo-doped CaO films (Bias set point 2.5 V). The electron transfer across the metal−oxide interface induces distinct shifts of the CaO band edges, providing insight into the charge state of the dopants.

defects are dislocation lines that compensate for the misfit strain between the oxide film and the Mo support. Point defects, on the other hand, are hardly detected in the STM, suggesting that the capping layer indeed inhibits segregation of

Received: December 6, 2011
Published: January 24, 2012

   dx.doi.org/10.1021/ja211396t | J. Am. Chem.Soc. 2012, 134, 2532−2534

the dopants to the surface. Only the spatial extension of oxide terraces was found to change for different doping procedures, with the smallest terrace sizes occurring for CaO_{Li}.

The presence of Mo dopants in the CaO films has been confirmed with Auger spectroscopy, revealing the characteristic Mo transitions at ∼200 eV kinetic energy. In contrast, the Li impurities could only be probed indirectly via their impact on the energy position of the CaO bands, as deduced from STM conductance measurements (Figure 1b). On pristine films, the valence (VB) and conduction band (CB) edges are detected at −5.0 and +2.0 V, respectively, demonstrating a substantial downshift of the midgap position with respect to the Fermi level. The shift reflects the development of a strong interface dipole between the basic CaO film and the electronegative Mo support, as discussed in a recent DFT study.[18] Upon Li doping, the bands move to higher energies, reaching VB = −4.0 V and CB = +3.0 V at 8% Li content. The rigid upshift is due to a back transfer of electrons from Mo to the CaO film in order to fill the holes created by Li^+ ions located on Ca^{2+} substitutional sites. As a result, the positive dipole at the CaO/Mo interface diminishes and the CaO midgap position moves closer to the Fermi level. The band shift is fully reversible, and the original situation is restored when removing the Li from the oxide film upon heating to 1050 K (Figure 1b, lower curve). Not surprisingly, the opposite effect is observed for CaO_{Mo}, as the Mo dopants adopt a higher charge state and release electrons to the lattice.[19] Transfer of these excess charges to the metal support reinforces the initial interface dipole and promotes a further downshift of the bands to VB = −5.5 V and CB = +1.5 V. We note that only dopants close to the interface participate in this electron transfer, while near-surface species retain their original charge state due to the large tunneling barrier to the Mo metal.

The latter might however be able to donate electrons to adsorbates. To explore this possibility, we have dosed small amounts of gold, which is a good electron acceptor, onto the doped CaO films. An electron transfer might be derived in this case from the equilibrium shape of the Au deposits, as negatively charged gold was found to grow into 2D islands on various oxide supports.[14,15] On pristine CaO, gold develops 3D deposits, as expected from its weak interaction with the wide-gap insulator (Figure 2a). The mean particle shape is described by an aspect ratio of (0.35 ± 0.10), a typical value for the Volmer−Weber regime (Figure 2e). Inserting 4% of Mo into the CaO matrix changes the particle shapes from 3D to 2D. The 2D deposits appear as faint depressions in the STM images, because electron transport is more efficient into the bare CaO than into the Au islands at high sample bias (Figure 2b). The reason for this contrast inversion is the presence of low-lying vacuum states with high electron transmissibility above the CaO surface that are not available above the metal islands.[15,20] The regular contrast with the Au deposits appearing bright is only revealed below 3.0 V sample bias; however low-bias tunneling through a 50 ML thick CaO film is challenging (Figure 2b, inset). The aspect ratio of Au islands on CaO_{Mo} films has been determined with (−0.07 ± 0.02) at 6.0 V sample bias, which corresponds to a Au monolayer.

Adding small amounts of Li to CaO_{Mo} strongly alters the observed growth behavior. As long as the Li content is lower than the one of Mo, most of the Au deposits remain 2D and only particles along the CaO dislocation lines switch back to a 3D geometry. This leads to a bimodal particle-shape distribution characterized by two well-separated maxima

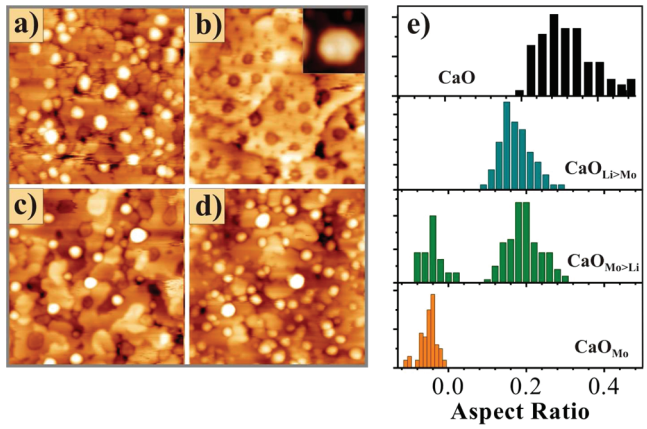

Figure 2. STM images of 0.5 ML Au deposited onto (a) pristine CaO; (b) doped with 4% Mo; (c) doped with 4% Mo + 2% Li; and (d) doped with 4% Mo + 8% Li (6.0 V, 50 × 50 nm^2). Note that monolayer Au islands in (b) and (c) appear as depressions at high sample bias. The typical contrast is only revealed in low bias images (3.0 V, see inset of b), which are however difficult to obtain on the insulating oxide film. (e) Histogram of aspect ratios for Au particles grown on the differently doped CaO films.

(Figure 2e). With increasing Li concentration, the fraction of 2D islands decreases with respect to the 3D deposits (Figure 2c). Once the Li doping level exceeds the one of Mo, the original shape distribution of bare CaO is restored and only the particle density is somewhat higher due to the lower surface quality of CaO_{LiMo} films. We note that pure Li doping has almost no effect on the Au growth characteristic.

The observed changes in the Au particle geometry on doped CaO films can be explained with charge-transfer processes between the dopants and the ad-metal.[21] Recent DFT calculations have shown that Mo impurities in a CaO host adopt a +2 charge state, though one of the four Mo 4d electrons occupies an energetically unfavorable t_{2g} state close to the CB edge.[19] This electron is prone to transfer to the Au 6s affinity level being at lower energy. As a result, the Mo dopant becomes oxidized while the Au atom takes a negative charge. The anionic gold features strong Coulomb and polaronic interactions with the CaO surface, resulting in a substantial metal−oxide adhesion. In an attempt to maximize this charge-mediated coupling, the gold increases its contact area with the oxide surface and spreads into monolayer islands. In contrast to Mo, Li is a charge acceptor as it lacks one valence electron with respect to the divalent Ca. It thus creates energetically costive holes in the 2p orbitals of adjacent O ions that can be filled by electrons from the Mo codopants. The presence of Li in CaO_{Mo} films therefore triggers charge-compensation effects between the dopants, reducing the number of electrons that are available for transfer into the Au deposits.[22,23] The absence of excess electrons now forces the gold to adopt its original 3D growth regime, in agreement with the experimental findings.

The geometry crossover affects primarily particles along the CaO dislocation lines, suggesting that the line defects are the preferred binding sites of Li. Alternatively, additional electron acceptors might be present along those defects, e.g. O vacancies or structural electron traps, which also disrupt the charge flow into the gold. We have no indication of positive Au charging if only Li dopants are present in the CaO films. While this observation might be unexpected at first glance, it is readily explained by alternative routes to remove the unfavorable holes

dx.doi.org/10.1021/ja211396t | J. Am. Chem.Soc. 2012, 134, 2532−2534

created by the Li dopants. The required electrons are provided by either O defects (F^0 or F^{2+} centers) or donor-type adsorbates in the rest gas, e.g. H_2 or H_2O.[17,23] In any case, the charge imbalance due to Li incorporation will be removed long before the Au interacts with the surface.

In conclusion, we have successfully tailored the shape of Au particles by doping a CaO support with Mo or Li impurities. Inserting overvalent Mo species leads to the growth of 2D metal islands that are stabilized by an electron transfer from the impurity ions. Codoping with Li effectively blocks this charge exchange, as excess electrons are trapped by O 2p-type holes created by the alkali dopants. Consequently, charge-compensated Li^+−Mo^{3+} ion pairs develop that are unable to modify the Au growth behavior. Our study elucidates how shaping of metal ad-particles might be possible via doping the oxide support. It also illustrates that codoping, being a widely proposed strategy in the catalytic literature, results in internal charge compensation that destroys the desired effect.

■ AUTHOR INFORMATION

Corresponding Author

nilius@fhi-berlin.mpg.de

Notes

The authors declare no competing financial interest.

■ ACKNOWLEDGMENTS

We are grateful to the DFG-Cluster of Excellence 'Unicat' for financial support and thank G. Pacchioni for many discussions.

■ REFERENCES

(1) Yan, W. F.; Chen, B.; Mahurin, S. M.; Schwartz, V.; Mullins, D. R.; Lupini, A. R.; Pennycook, S. J.; Dai, S.; Overbury, S. H. *J. Phys. Chem. B* **2005**, *109*, 10676−10685.

(2) Chen, M. S.; Goodman, D. W. *Acc. Chem. Res.* **2006**, *39*, 739−746.

(3) Hashmi, A. S. K.; Hutchings, G. J. *Angew. Chem., Int. Ed.* **2006**, *45*, 7896−7936.

(4) Risse, T.; Shaikhutdinov, S.; Nilius, N.; Sterrer, M.; Freund, H. J. *Acc. Chem. Res.* **2008**, *41*, 949−956.

(5) Chen, M. S.; Goodman, D. W. *Science* **2004**, *5694*, 252−255.

(6) Herzing, A. A.; Kiely, C. J.; Albert, A. F.; Landon, P.; Hutchings, G. J. *Science* **2008**, *321*, 1331−1335.

(7) Mostafa, S.; Behafarid, F.; Croy, J. R.; Ono, L. K.; Li, L.; Yang, J. C.; Frenkel, A. I.; Roldan Cuenya, B. *J. Am. Chem. Soc.* **2010**, *132*, 15714−15719.

(8) Molina, L. M.; Hammer, B. *Appl. Catal., A* **2005**, *291*, 21−31.

(9) Lin, X.; Yang, B.; Benia, H.-M.; Myrach, P.; Yulikov, M.; Aumer, A.; Brown, M. A.; Sterrer, M.; Bondarchuk, O.; Kieseritzky, E.; Rocker, J.; Risse, T.; Gao, H.-J.; Nilius, N.; Freund, H.-J. *J. Am. Chem. Soc.* **2010**, *132*, 7745−7749.

(10) Green, I. X.; Tang, W. J.; Neurock, M.; Yates, J. T. *Science* **2011**, *333*, 736−739.

(11) Lisiecki, I.; Billoudet, F.; Pileni, M. P. *J. Phys. Chem.* **1996**, *100*, 4160−4166.

(12) Koplitz, L. V.; Dulub, O.; Diebold, U. *J. Phys. Chem. B* **2003**, *107*, 10583−10590.

(13) Fuks, D.; Zhukovskii, Y. F.; Kotomin, E. A.; Ellis, D. E. *Surf. Sci.* **2006**, *600*, L99−L104.

(14) Pacchioni, G.; Giordano, L.; Baistrocchi, M. *Phys. Rev. Lett.* **2005**, *94*, 226104.

(15) Nilius, N. *Surf. Sci. Rep.* **2009**, *64*, 595−659.

(16) Shao, X.; Myrach, P.; Nilius, N.; Freund, H.-J. *J. Phys. Chem. C* **2011**, *115*, 8784−8789.

(17) Myrach, P.; Nilius, N.; Levchenko, S.; Gonchar, A.; Risse, T.; Dinse, K.-P.; Boatner, L. A.; Frandsen, W.; Horn, R.; Freund, H.-J.; Schlögl, R.; Scheffler, M. *ChemCatChem* **2010**, *2*, 854−862.

(18) Giordano, L.; Cinquini, F.; Pacchioni, G. *Phys. Rev. B* **2006**, *73*, 045414.

(19) Shao, X.; Prada, S.; Giordano, L.; Pacchioni, G.; Nilius, N.; Freund, H. -J. *Angew. Chem., Int. Ed.* **2011**, *50*, 10096−10115.

(20) Binnig, G.; Frank, K. H.; Fuchs, H.; Garcia, N.; Reihl, B.; Rohrer, H.; Salvan, F.; Williams, A. R. *Phys. Rev. Lett.* **1985**, *55*, 991−995.

(21) Chrétien, S.; Metiu, H. *J. Chem. Phys.* **2008**, *128* (044714), 1−13.

(22) Li, B.; Metiu, H. *J. Phys. Chem. C* **2010**, *114*, 12234−12244.

(23) Hu, Z.; Li, B.; Sun, X. Y.; Metiu, H. *J. Phys. Chem. C* **2011**, *115*, 3065−3074.